



Letters

Template-free fabrication of vertically-aligned polymer nanowire array on the flat-end tip for quantifying the single living cancer cells and nanosurface interaction



Biran Wang^{a,1}, Liming Wang^{a,1}, Xi Li^b, Yuchen Liu^a, Zimeng Zhang^a, Erik Hedrick^b, Stephen Safe^b, Jingjing Qiu^c, Guohui Lu^d, Shiren Wang^{a,*}

^a Department of Industrial & Systems Engineering, Texas A&M University, College Station, TX 77843, United States

^b Department of Veterinary Physiology & Pharmacology, Texas A&M University, College Station, TX 77843, United States

^c Department of Mechanical Engineering, Texas Tech University, Lubbock, TX 77409, United States

^d Department of Biomedical Sciences, University of South Carolina School of Medicine, Greenville, SC 29605, United States

ARTICLE INFO

Article history:

Received 16 March 2018

Accepted 18 March 2018

Available online 19 March 2018

ABSTRACT

We fabricated vertically aligned polyaniline (PANI) nanowire arrays on flat-end AFM tips via template-free methods. 4-Aminothiophenol was used for tailoring the nucleation size, chain propagation and orientation of the PANI nanowires. The microscopy characterization indicated that diameter was centered at a mean of 33.7 nm with a standard deviation of 6.5 nm, and length was centered at a mean of 50.3 nm with a standard deviation of 7.6 nm. PANI nanowire arrays are non-toxic, low-cost, and tunable, and thus PANI nanowire-grown tips could perfectly simulate different nanosurfaces. Via the force spectroscopy, we demonstrate the feasibility in real-time quantifying the nanostructure-cell interactions at the single cell level with high reliability and accuracy. This work will enable a new tool in precisely quantifying the interactions of single living cells and nanosurface, and thus opens a new door to understand how single living cells sense and respond to the specific nanostructures.

© 2018 Society of Manufacturing Engineers (SME). Published by Elsevier Ltd. All rights reserved.

1. Introduction

Cell adhesion is a fundamental and critical issue for versatile biological processes, such as cell separation, production or migration [1]. Cell adhesion could help cells to identify numerous extracellular signals regarding the chemistry, geometry and physical characteristics of the matrix [2,3]. Nanostructured surfaces have been extensively used in tissue engineering and regenerative medicine [4], and also emerged as a promising biosensing platform to promote the cellular interactions with internal and external mediators [5]. Recent studies have shown that nanostructured surfaces greatly improved cell adhesion. Variable nanostructures have been synthesized and their interaction with cells was examined to disclose the nanostructure effect on the adhesion [6,7]. However, those results are based on the population adhesions, where numerous cells are incubated on the nanostructured substrate and then the cell adhesion is quantified by counting the cell numbers (or expansion of cell spreading areas) on the substrate based on the shearing-flow fluid [8].

Precise measurement of single-cell adhesion is critical to understand how cells sense and respond to the nanostructure [9]. AFM is one of the simplest techniques for characterization and manipulation of living cells in a physiology medium with a nanoscale resolution. No special treatments are needed for preparing the AFM samples. Few bottom-up nanotechniques have been attempted to fabricate nanostructures on AFM tips. Mino et al. evaporated Ag on the silicon cantilever and produced *random* Ag nanostructures around the tip apex, where tip end size is <50 nm [10]. Sanders et al. also deposited *random* gold nanoparticles on the AFM tip via electrochemical deposition [11,12]. Kharintsev et al. used electrochemical-etching method to produce *random* nanostructures on the AFM tip surfaces [13]. Leiterer et al. randomly attached silver nanoparticles on AFM tips by dielectrophoresis [14]. Uebel et al. used a wet-chemical etching and mechanical cleaving technique to fabricate gold nanotips [15]. Weber-Bargioni et al. and some other groups employed focused-ion-beam machining to fabricate high-aspect ratio AFM tips [16–20]. Denisyuk et al. reported the nanoparticle pickup method under electron beam to make the spherical metallic nanoshell and a small metallic nanoparticle (“nanoknob”) situated on tip’s surface [21]. However, those nanostructures fabricated on the AFM tips are random and lack a long-range order for well-controlled morphology,

* Corresponding author.

E-mail address: s.wang@tamu.edu (S. Wang).

¹ These authors contributed equally to this work.

and thus are not suitable for measurement of the single tumor cell adhesion due to the lack of scientific rigor and reproducibility. Recently, Pyrgiotakis et al. attached various types of oxide nanoparticles on the sharp tips to quantify the real time nanoparticle–cell interactions in physiological media [22], but the nanoparticles on the sharp tips are still random. Acerbi et al fabricated the cylindrical flat end-AFM tips with $\sim 1 \mu\text{m}^2$ cross-section area by FIB [23], and the flat end surface would be a good option to transform to one dimensional nanostructured surface. Unfortunately, it's still too small to globally quantify the cell adhesion in comparison to the size of the cells ($\sim 100 \mu\text{m}$).

To actively investigate the behavior of cell on the nanostructured surface, for the first time we create an ordered polyaniline (PANI) nanowire arrays on flat-end AFM tips, and systematically quantify the nanostructure–cell interactions at the single cell level in real time with high reliability and accuracy. Vertically aligned PANI nanowire arrays have been reported with different diameters and length on kinds of substrates [24]. They are non-toxic,

low-cost, and highly stable, and thus are very promising for studying single cell adhesion on the nanostructures.

2. Experimental

Aniline (ANI, $\geq 99.5\%$), 4-Aminothiophenol (4-ATP, 97%) and perchloric acid (HClO_4 , 60%) were purchased from Sigma Aldrich and used as received without further purification. Flat-end AFM tips (plateau diameter: 8–12 μm , plateau height: 15 μm , the length of cantilever: 450 μm , the width of cantilever: 50 μm) were purchased from NanoAndMore.

Polyaniline (PANI) nanowire arrays were prepared on AFM tips by the electrochemical polymerization method. Briefly, AFM tip was coated by 10 nm thick Au layer by thermal evaporation and then immersed into 1 mM 4-ATP/ethanol solution for 5 min. This modified AFM was used as a positive electrode during the electrochemical polymerization reaction, while a Pt wire was used as a

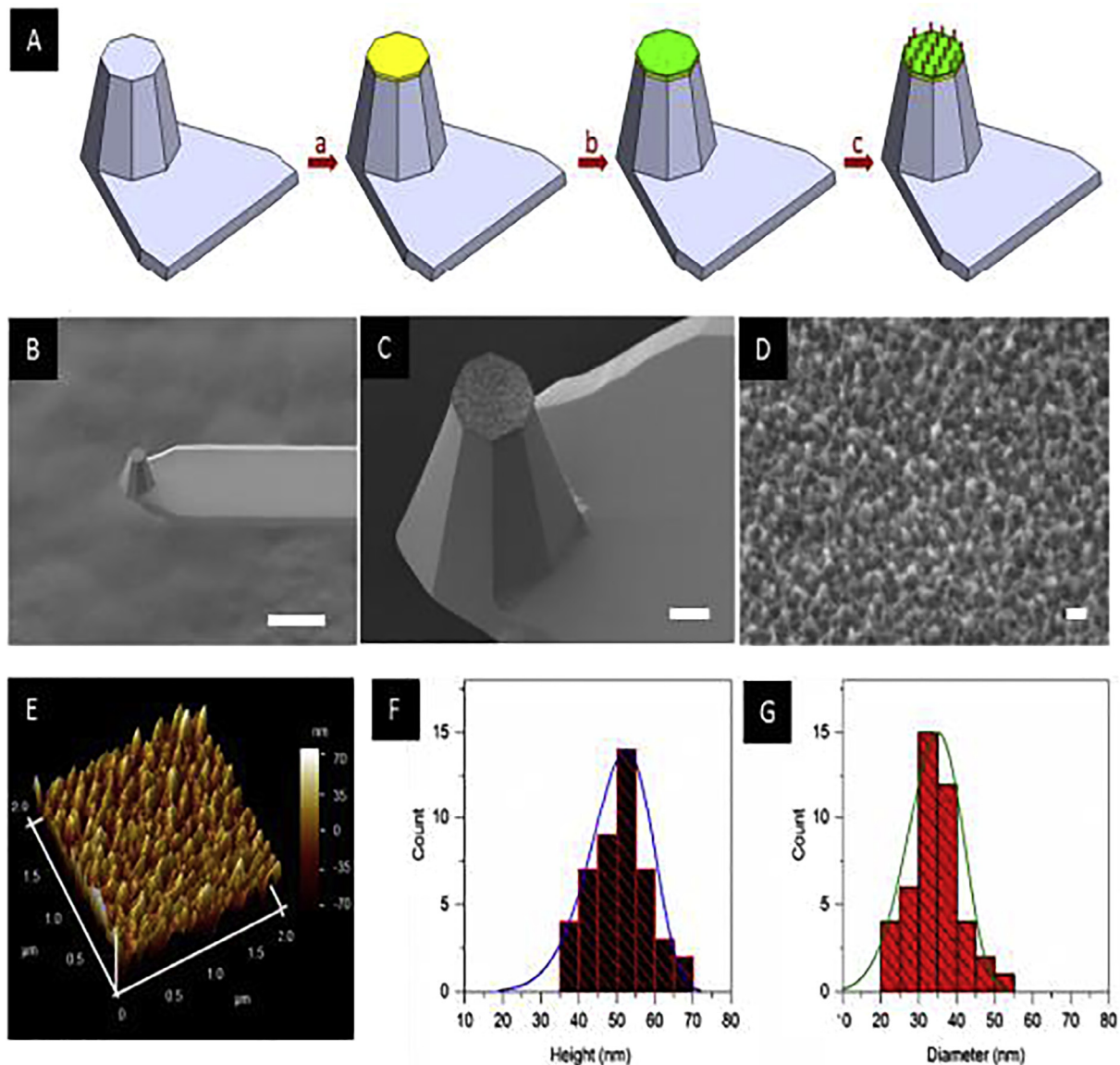


Fig. 1. Manufacturing nanostructured flat-end AFM tip. (A): Schematic representation of creation process (a: Deposition of the 10 nm gold coating by thermal evaporation, b: 4-ATP nucleation, c: Polyaniline (PANI) nanowire growth). (B–D): SEM images of the flat-end AFM tips and as-created nanostructure. The diameter of the flat end surface is around 10 μm , scale bars are 30 μm (B), 5 μm (C), and 100 nm (D), respectively. (E): AFM image of the vertical-aligned nanowire array on the flat-end tip. (F and G): Distribution of diameter and height of nanowires.

negative electrode. Then a certain volume of mixed solution containing 0.1 M ANI and 1 M HClO₄ was injected into the container. A Keithley 2400 was used to supply constant current (0.2 μ A). The polymerization reaction was conducted under a current density of 10 μ A/cm² at room temperature for 1 h. After the reaction, AFM tips were rinsed with ethanol for several times to remove any residuals. Finally, the washed AFM tips were dried in air for further use. The as-prepared AFM tip with PANI nanowire arrays was characterized by Raman spectrometer (Jobin-Yvon HORIBA LabRAM HR800 instrument coupled to an Olympus BX41 microscopy, $\lambda_{exc.}$ = 514.5 nm), SEM (JEOL JSM-7500F) and AFM (Bruker, contact mode).

AFM adhesion experiments were performed on a BioScope II scanner (Bruker Inc.) integrated with a Nikon TE2000 inverted optical microscope.

3. Results

The fabrication process is illustrated in Fig. 1A. 4-ATP assisted template-free synthesis of PANI nanowire arrays was carried out on the flat-end surface of the AFM probe. The morphology of as-prepared AFM tip with PANI nanowire arrays was characterized by SEM and AFM, respectively, as showed Fig. 1B–E. The length and diameter distribution indicated that diameter was centered at a mean of 33.7 nm with a standard deviation of 6.5 nm, and length was centered at a mean of 50.3 nm with a standard deviation of 7.6 nm, as shown in Fig. 1F and G. Raman characterization was also carried out to confirm the successful fabrication of PANI nanowire arrays on the tip. As shown in Fig. 2, several characteristic peaks of PANI were observed including the C–H bending vibration of the quinoid/benzenoid rings at 1168 cm^{-1} , C–N+ vibration of delocalized polaronic structures at 1336 cm^{-1} , C=N stretching of the quinoid rings at 1510 cm^{-1} , C–C stretching of the benzenoid rings at 1598 cm^{-1} , and vibration of delocalized polarons at 1378 cm^{-1} and 1636 cm^{-1} .

After successfully creating the nanostructured surface on the flat-end tip, the single cell adhesion experiment using this tip has been conducted. We tested two different type of human breast cancer cells, MDA-MB-231 and SKBR3, and one normal human breast epithelial cell, MCF-10A. To make every test under the same condition, AFM has been set to apply a constant force to each cell. As illustrated in Fig. 3A, the nanostructured surface tip placed on top of the single cells, the cell adhesion can be quantified by the

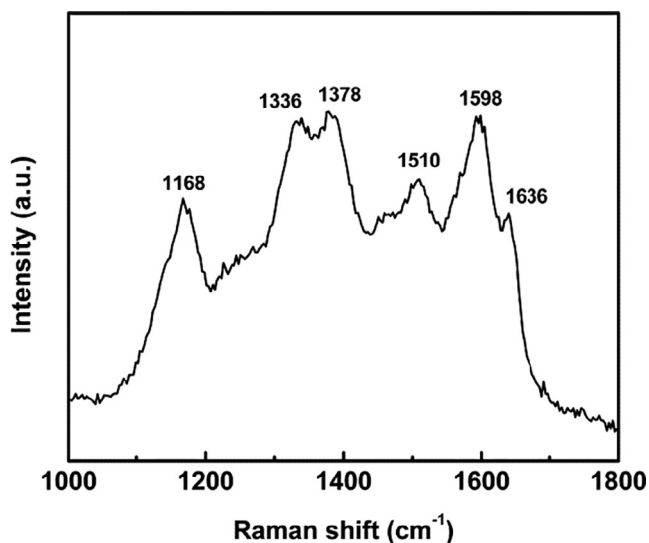


Fig. 2. Raman spectrum of as-prepared PANI nanowire arrays.

approach-retract of the AFM tip towards the cell in the vertical direction, (the approach and retract curves are represented by blue and red, respectively). Briefly, the tip applies a constant and default force upon the cell surface that leads to the sample indentation and cantilever deflection, once the tip meets its maximum indentation, it withdraws from the cell surface. The adhesion force between the sample and the AFM tip hampers tip retraction. Therefore, these unbinding forces or the adhesion strength can be taken directly from the retracting part of the force-distance curve, as indicated in Fig. 3C.

The adhesion force of single cancer cells with the nanostructured surface was precisely measured. Firstly, on each cell surface, we choose 4 test locations as indicated in Fig. 3B, and at each point, 5 measurements have been repeated. The result demonstrates that the measurements are highly accurate, as shown in Fig. 3D, the measurements implemented on the one MDA-MB-231 cell, and each test point has a very small deviation (less than 10%). On the other hand, there is a huge difference between those points, the average of 4 test points are 9.2 nN, 6.4 nN, 9.1 nN, and 12.1 nN, respectively. The variation is significant, the maximum adhesion force is almost doubled compared to the minimum one (12.1 nN–6.4 nN). It indicated that the cancer cell surface is extremely heterogeneous.

It's well known that many receptors on cell surfaces contribute to the adhesion, such as integrins, cadherins, and other adhesion molecules. The consensus is that integrins play a most important role in the cell adhesion receptors, which demonstrate 24 different α - β combinations. When cells start to adhere to a substrate, the first step is to create a close contact between the plasma membrane and the substrate. Once a mature adhesion has been established, the integrin-based focal adhesions providing anchorage to the substrate are strongly connected to the actin cytoskeleton, the main basis of cell shape and structure. Focal adhesions anchor cells to the substrate and can facilitate both mechanical and biochemical interaction; therefore, they are the sites at which forces are transmitted to the substrate.

To understand the mechanism of single cell and nanostructured tip interactions, we also investigate the cell adhesion in the molecular level. Firstly a regular AFM tip was functionalization by RGD as previously described [25,26]. Briefly, The N-terminus of the RGD peptide was grafted to a regular tip by covalent bonds, and the grafted RGD enable the tip to sense biological characteristics. Via this RGD coated tip, the RGD-recognized integrins can be visualized on the cell surface, as shown in Fig. 3E and F. As a result, that the spatial distribution of the RGD-recognized integrins was mapped and indicated the diverse arrangements of unbinding forces on the MDA-MB-231 cell. Even on the same type of cell surface, the force map seems very different (adhesion force is proportional to the brightness). The map of integrin on cell surface provides an insight to understand the individual cell interactions with the nanosurface.

The variation of those adhesions is up to 50%, but their average adhesion of different cells (the same type) are rather close, as shown in Fig. 4A. Four different MDA-MB-231 cells were randomly selected and compared, and the averages of adhesion strength of each cell are found to 11.1 nN, 9.6 nN, 10.5 nN, 9.1 nN, respectively, indicating only 9% of variation. To further verify this method, we tested another type of breast cancer cell SKBR3, and compare two breast cancer cells to a normal breast cell, MCF-10A. The results of adhesion between cells and regular flat-end tip or nanostructured flat-end tip are shown in Fig. 4B. The results showed that adhesion force is very low using a regular flat-end tip, either on cancer cells or normal cell (red). As a result, such regular tip is not able to distinguish the cancer cells and the normal health cells. However, when nanostructured surface flat-end tip is used, significant adhesion differences were found between cancer cells and

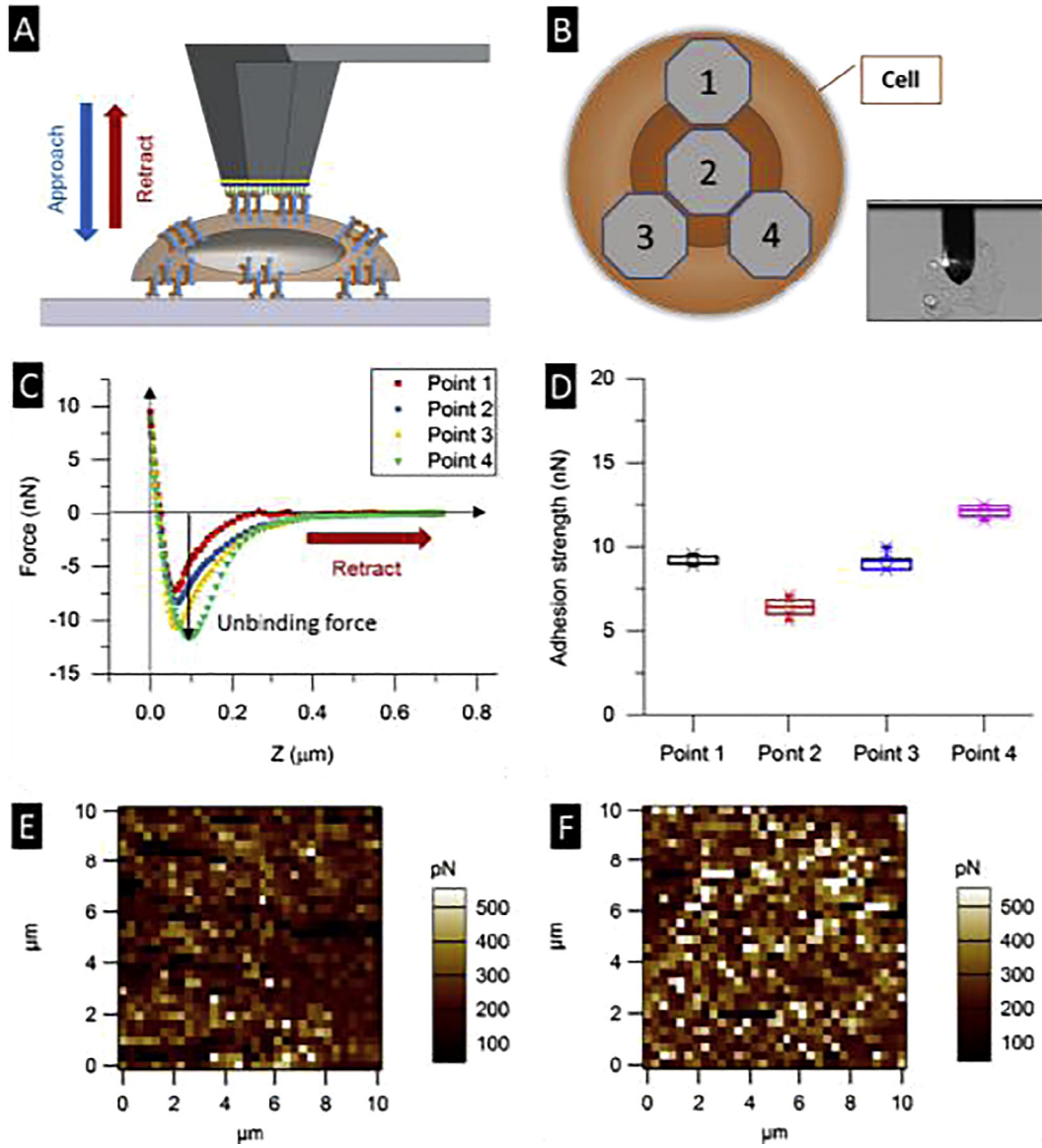


Fig. 3. Detection of adhesion force of single living cell by nanostructured flat-end AFM tip. (A) Illustration of measurement mechanism, (B) Illustration of measurement location, 4 different test points on each cell have been taken, the locations were practically the same for each cell, (C) Unbinding force of 4 different test points on one cancer cells using nanostructured flat-end AFM tip. (D) The adhesion strength of one cancer cell; 4 test points at the location as indicated in B, were analyzed and each point takes 5 measurements. (E and F) AFM force maps of RGD-integrin binding on one breast cancer cell; the maps were taken at the perinuclear (E) and peripheral regions (F).

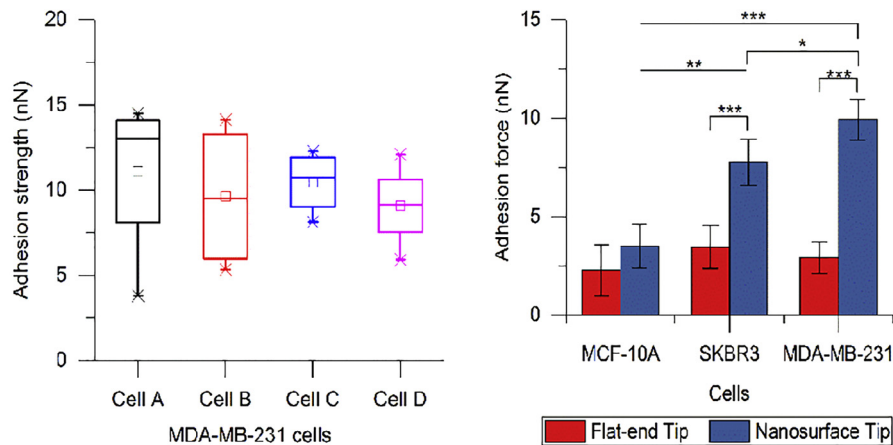


Fig. 4. Adhesion force of different cells, same type (A) and comparison of different breast cell types (B).

normal cells, or between two cancer cells (blue). Furthermore, compared to non-treated tip, the adhesion forces of cancel on nanostructured surface tip are almost tripled, while no significant change has been observed in normal cells. Therefore, it could be possible to use novel nanostructured tip for isolation or detection of cancer cells, only based on the quantification of adhesion force. This method is label-free and universal, and could open a new door for the adhesion study.

4. Conclusions

In summary, ordered nanostructures were fabricated on the flat-end tip and its feasibility in single-cell adhesion study was demonstrated. Such direct measurement of single cell adhesion using novel nanostructure tips opens a new door to single cell study, particularly, in understanding the heterogeneity of the cancer cells.

Acknowledgements

We are grateful to the support from Texas A&M University and TEES startup funds, AmCare Genomics Laboratory, and NSF grants (#1634858).

References

- [1] Engler AJ, Sen S, Sweeney HL, Discher DE. *Cell* 2006;126:677–89.
- [2] Geiger B, Spatz JP, Bershadsky AD. *Rev Mol Cell Biol* 2009;10:21–33.
- [3] Berrier AL, Yamada KM. *J Cell Physiol* 2007;213:565–73.
- [4] Geckil H, Xu F, Zhang X, Moon S, Demirci U. *Nanomed* 2010;5:469–84.
- [5] Smith IO, Liu XH, Smith LA, Ma PX. *Wiley Interdiscip Rev Nanomed Nanobiotechnol* 2009;2009(1):226–36.
- [6] Dolatshahi-Pirouz A, Jensen T, Kraft DC, Foss M, Kingshott P, Hansen JL, et al. *ACS Nano* 2010;4:2874–82.
- [7] Abdul Kafi M, El-Said WA, Kim T-H, Choi J-W. Cell adhesion, spreading, and proliferation on surface functionalized with RGD nanopillar arrays. *Biomaterials* 2012;33:731–9.
- [8] Wang S, Liu K, Liu J, Yu ZT-F, Xu X, Zhao L, et al. Highly Efficient Capture of Circulating Tumor Cells by Using Nanostructured Silicon Substrates with Integrated Chaotic Micromixers. *Angew Chem Int Ed* 2011;50:3084–8.
- [9] Sniadecki NJ, Desai RA, Ruiz SA, Chen CS. *Nanotechnology for Cell-Substrate Interactions. Ann Biomed Eng* 2006;34:59–74.
- [10] Mino T, Saito Y, Verma P. Quantitative analysis of polarization-controlled tip-enhanced raman imaging through the evaluation of the tip dipole. *ACS Nano* 2014;8:10187–95. <https://doi.org/10.1021/nn5031803>.
- [11] Sanders A, Bowman RW, Zhang L, Turek V, Sigle DO, Lombardi A, et al. Understanding the plasmonics of nanostructured atomic force microscopy tips. *Appl Phys Lett* 2016;109:153110. <https://doi.org/10.1063/1.4964601>.
- [12] Sanders A, Zhang L, Bowman RW, Herrmann LO, Baumberg JJ. Facile fabrication of spherical nanoparticle-tipped afm probes for plasmonic applications. *Part Part Syst Charact* 2015;32:182–7. <https://doi.org/10.1002/ppsc.201400104>.
- [13] Kharintsev SS, Hoffmann GG, Fishman AI, Salakhov MK. *J Phys Appl Phys* 2013;46:145501.
- [14] Leiterer C, Wünsche E, Singh P, Albert J, Köhler JM, Deckert V, et al. *Anal Bioanal Chem* 2016;408:3625–31.
- [15] Uebel P, Bauerschmidt ST, Schmidt MA, St.J. Russell P. A gold-nanotip optical fiber for plasmon-enhanced near-field detection. *Appl Phys Lett* 2013;103:021101. <https://doi.org/10.1063/1.4813115>.
- [16] Weber-Bargioni A, Schwartzberg A, Schmidt M, Harteneck B, Ogletree DF, Schuck PJ, et al. Functional plasmonic antenna scanning probes fabricated by induced-deposition mask lithography. *Nanotechnology* 2010;21:065306. <https://doi.org/10.1088/0957-4484/21/6/065306>.
- [17] Fleischer M, Weber-Bargioni A, Altoe MVP, Schwartzberg AM, Schuck PJ, Cabrini S, et al. Gold Nanocone Near-Field Scanning Optical Microscopy Probes. *ACS Nano* 2011;5:2570–9. <https://doi.org/10.1021/nn102199u>.
- [18] Maouli I, Taguchi A, Saito Y, Kawata S, Verma P. Optical antennas for tunable enhancement in tip-enhanced Raman spectroscopy imaging. *Appl Phys Express* 2015;8:032401. <https://doi.org/10.7567/APEX.8.032401>.
- [19] Huth F, Chuvilin A, Schnell M, Amenabar I, Krutokhvostov R, Lopatin S, et al. Resonant antenna probes for tip-enhanced infrared near-field microscopy. *Nano Lett* 2013;13:1065–72. <https://doi.org/10.1021/nl304289g>.
- [20] Zou Y, Steinvurzel P, Yang T, Crozier KB. Surface plasmon resonances of optical antenna atomic force microscope tips. *Appl Phys Lett* 2009;94:171107. <https://doi.org/10.1063/1.3116145>.
- [21] Denisuyuk AI, Tinskaya MA, Petrov MI, Shelaev AV, Dorozhkin PS. Tunable optical antennas based on metallic nanoshells with nanoknobs. *J Nanosci Nanotechnol* 2012;12:8651–5. <https://doi.org/10.1166/jnn.2012.6477>.
- [22] Pyrgiotakis G, Blattmann CO, Demokritou P. *ACS Sustain Chem Eng* 2014;2:1681–90.
- [23] Acerbi I, Luque T, Giménez A, Puig M, Reguart N, Farré R, et al. *PLoS ONE* 2012;7:e32261.
- [24] Li L, Qiu J, Wang S. Three-dimensional ordered nanostructures for supercapacitor electrode. *Electrochim Acta* 2013;99:278–84.
- [25] Wang B, Guo P and Auguste D T *Biomaterials*, 2015,57 161–8.
- [26] Guo P, Wang B, Liu D, Yang J, Moses M, Auguste D. *Cancer Res*. 2016;76:2207–8.